Journal of Science: Advanced Materials and Devices 7 (2022) 100401

Contents lists available at ScienceDirect

Journal of Science: Advanced Materials and Devices

journal homepage: www.elsevier.com/locate/jsamd

Original Article

Metamaterial with sign-toggling thermal expansivity inspired by Islamic motifs in Spain

Teik-Cheng Lim

School of Science and Technology, Singapore University of Social Sciences, Singapore

A R T I C L E I N F O

Article history:
Received 7 April 2021
Received in revised form
25 October 2021
Accepted 2 November 2021
Available online 9 November 2021

Keywords:
Composites
Material structure
Smart materials
Thermal properties

A B S T R A C T

A metamaterial design is introduced herein, which exhibits negative thermal expansion during heating but reverses into positive thermal expansion during cooling with respect to the reference temperature. The metamaterial is inspired by geometric patterns found at the Alhambra Palace and the Great Mosque of Cordoba and designed using bimetallic strips. Although hidden in the original state at the reference temperature, these Islamic geometrical patterns are fully manifested when a temperature change occurs. Based on the carbon-steel and the brass-steel bimetallic strips, which are the most commonly used metallic layers for the bimetallic strips, results indicate that the magnitude of the effective coefficient of thermal expansion (CTE) is linearly correlated to the change in temperature. Therefore, this metamaterial is beneficial not only for the ability to switch its effective CTE sign, but also to allow its CTE magnitude to be altered by the environmental temperature without active control.

1. Introduction

Metamaterials are artificially-designed materials at the micro-structural level to achieve desired overall behavior not from the base materials but due to their geometrical properties. In the case of mechanical metamaterials, this principle is applicable for most materials that can be (i) micro-machined, casted, kirigami-processed, 3D-printed and any other precision manufacturing such that (ii) the final microstructural geometry undergoes the desired deformation mechanism pathway. Limitations, therefore, exist for materials that cannot be precision processed to achieve the required micro-lattice geometry and for cases where the mechanical properties of the base material are either too compliant or too stiff to deform according to the desired mechanism. This paper explores a type of metamaterial that exhibits negative thermal expansion (NTE) properties upon heating but converts to a conventional, or positive thermal expansion, the material upon cooling. As such, the metamaterial persistently experiences thermal contraction regardless of whether the environmental temperature increases or decreases. Materials typically possess a positive coefficient of thermal expansion (CTE), i.e. they expand and contract resulting from heating and cooling, respectively. Conversely, NTE materials behave in the opposite manner – they shrink upon heating but enlarge upon cooling. Although NTE materials are rare in comparison to conventional ones, it is even rarer to stumble upon materials that exhibit both positive and negative CTE depending on the environmental condition. For example, NTE materials exist naturally over various temperature ranges, such as ZrV_2O_7 [1], $AlPO_4$–17 [2] and chabazite [3], but no such naturally occurring materials exist for sign-switchable CTE. In recent years, metamaterials with properties being tunable from positive to negative have been achieved in terms of magnetoresistance [4], photoconductivity [5] and crystal lenses [6], to name a few. It has, however, been proven that artificial material systems with positive or negative CTEs are achievable by deliberate design of the material microstructure [7,8].

Although the negativity of material properties permits the design of novel materials and structures that can function in specific ways that are unattainable by conventional materials, there are cases where it is beneficial for materials to possess negative characteristics under specific environmental conditions but reverse to positive attributes under another environmental condition. Toggling between positive and negative properties was made possible by designing microstructures that exhibit zero effective properties such that prescription of positive or negative changes in the stimuli gradually re-shapes the microstructural geometries in an opposing manner to give effective properties of opposing signs [9,10]. Another approach is via microstructural duality, in which there are effectively two opposing sets of functioning

E-mail address: alan_tc_lim@yahoo.com.

Peer review under responsibility of Vietnam National University, Hanoi.

https://doi.org/10.1016/j.jsamd.2021.11.003

microstructures within the over-designed microstructure [11,12], with the contrasting set taking precedence under opposing stimuli. Of late, a few metamaterials designs have been conceptualized by drawing inspiration from Islamic geometric patterns [13–19]. Inspired by the Islamic geometric patterns at the Alhambra Palace and at the Great Mosque of Cordoba (Fig. 1), this paper proposes a metamaterial with sign-toggling capability based on bimetallic strips without the need to interchange the positions of the bimetallic layers. This metamaterial in its original state is illustrated in Fig. 2 (top center) where straight bimetallic strips are built into rigid square blocks. Regardless of whether the temperature increases or decreases, the curving of the bimetallic strips causes the distance between the rigid square blocks to shorten, thereby resulting in overall shrinkage. This causes NTE during heating (Fig. 2 top right), but positive CTE during cooling (Fig. 2 top left) until the terminal states shown in Fig. 2 (bottom) is attained. In other words, the considered metamaterial possesses the capability to switch the sign of its CTE between positive and negative values ($\alpha_{eff} < 0$ for $dT > 0$ but $\alpha_{eff} > 0$ for $dT < 0$) without the need to swap the positions of the bimetallic layers of high and low CTEs. One can see that the Islamic geometric patterns are revealed upon a change in temperature. Precisely, the intermediate state of thermally-induced curvature shown in Fig. 2 (top right and top left) correspond to the tile mosaic patterns of the Alhambra Palace shown in Fig. 1 (top left), while the terminal state of the thermal deformation furnished in Fig. 2 (bottom) match the pierced screen pattern at the Great Mosque of Cordoba exhibited in Fig. 1 (bottom left). Note that the only difference in the microstructural geometry between

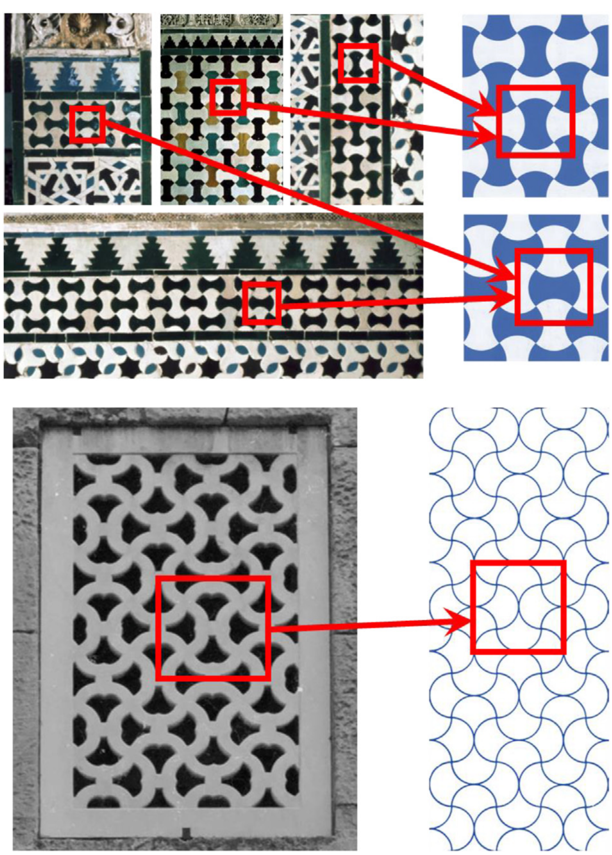

Fig. 1. Inspiration from Islamic geometric patterns at the tile mosaics of Alhambra Palace (top left) and its special case at a pierced screen of Cordoba's Great Mosque (bottom left) with their idealized drawings (right column).

heating and cooling, as represented by Fig. 2 (right) and (left), is that the layer with higher CTE (indicated in yellow) in the bimetallic strip becomes convex and concave under heating and cooling, respectively. The similarity in the resulting curvatures leads to an equal overall plane area under the same magnitude of temperature change. The difference in the arc length due to heating and cooling has been proven to be negligible [20].

2. Analysis

For a straight bimetallic strip of thickness h, consisting two metals of Young's modulus E_1 and E_2 with contrasting CTE α_1 and α_2, a change in temperature dT induces a radius of curvature r on the bimetallic strip such that the curvature can be expressed as (e.g. [21])

$$\frac{1}{r} = \frac{(\alpha_1 - \alpha_2)dT}{\frac{h}{2} + \frac{2}{h}(E_1 I_1 + E_2 I_2)\left(\frac{1}{E_1 h_1} + \frac{1}{E_2 h_2}\right)} \tag{1}$$

where $I_1 = h_1^3/12$ and $I_2 = h_2^3/12$ are the second moment areas of layer 1 and layer 2, with h_1 and h_2 being the corresponding thicknesses of the respective layers. The curvature model assumes that the bimetallic strip—as well as the individual bonded layers within—are sufficiently thin in comparison to their length, i.e. the length is assumed to be about two orders higher than the thickness, such that the bimetallic strip bends according to the Kirchhoff beam theory. For the special case of equal layer thickness $h_1 = h_2 = h/2$, Eq. (1) reduces to

$$\frac{1}{r} = \frac{24(\alpha_1 - \alpha_2)dT}{h\left(14 + \frac{E_1}{E_2} + \frac{E_2}{E_1}\right)} \tag{2}$$

Although further simplification can be obtained for layers of equal Young's modulus, no attempt is made herein because the current paper will adopt commonly used combination of metals in the bimetallic strips that are employed in practice due to their feasibility in being well-bonded with one another.

Fig. 3 (top left) shows a unit cell for the composite metamaterial under consideration at the original state whereby the rigid square connectors are indicated in red, and possess sides of dimension h to coincide with the thickness of the bimetal strip, while each bimetallic strip possesses a length of l. The center of the rigid square block is in the same plane as the interface of the bimetal strip due to equal thickness of both layers. Let layer 1 and layer 2 be made from materials of higher and lower CTEs, as indicated in yellow and green, respectively, in Fig. 3 (top right), then the unit cell deforms into the shape shown in Fig. 3 (bottom left) upon heating due to the differential extent of thermal strain. The deformation reverses to the schematic illustrated in Fig. 3 (bottom right) upon cooling from the original state. The effective CTE, α_{eff} can be obtained from the definition of thermal strain $\varepsilon = \alpha dT$, i.e. $\alpha_{eff} = \varepsilon_{eff}/dT$. Due to the large deformation encountered, the definition of infinitesimal strain $\varepsilon = dL/L_0$ (for a change in length dL from its original length L_0) is not used. Instead, we consider the infinitesimal strain $d\varepsilon = dL/L$ so as to obtain the total strain $\varepsilon = \int d\varepsilon = \ln(L_f/L_0)$ where L_0 and L_f are the original and final lengths, respectively. With reference to Fig. 3 (top left), let $L_0 = l_h + h$ be the distance between the centers of two nearest rigid square blocks measured either horizontally or vertically. Upon thermally-induced deformation, the distance between the centers of two nearest square blocks become $L_f = 2r \sin\theta + h\cos\theta$ where r, the radius of curvature indicated in Fig. 3 (bottom), is described by Eq. (2) for bimetals of

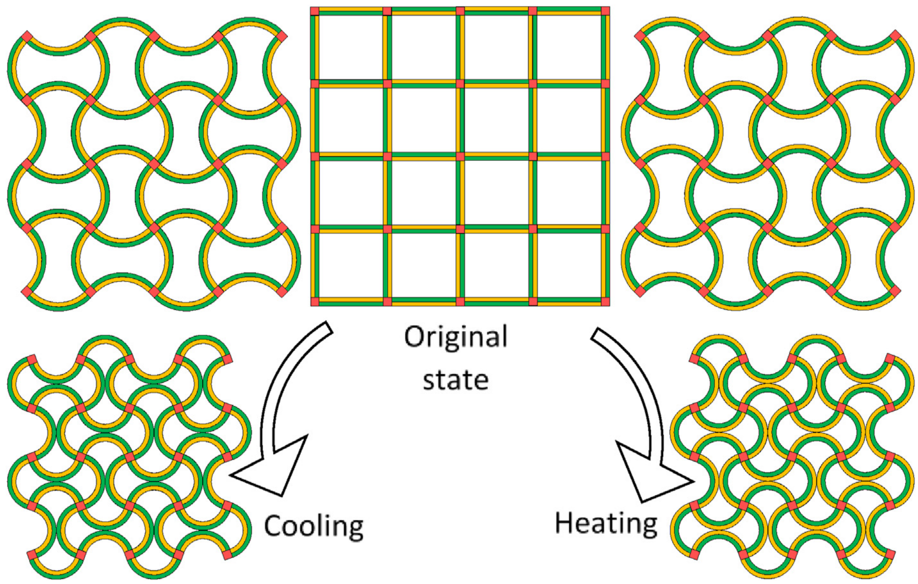

Fig. 2. The composite metamaterial considered herein in its original state (top center) undergoing intermediate contraction (top left and top right) to mimic the Islamic geometric pattern of Fig. 1 (top) and final stage of contraction (bottom) to mimic the Islamic geometric pattern of Fig. 1 (bottom).

equal layer thickness. Substituting L_f and L_0 into the total strain ε, we have the effective strain

$$\varepsilon_{eff} = \ln \frac{2 \sin \theta + \frac{h}{l}\frac{l}{r}\cos \theta}{\frac{l}{r}\left(1 + \frac{h}{l}\right)} \tag{3}$$

where h/l signifies the dimensionless thickness of the bimetallic strip. Taking the bimetallic strip length l as the mid-surface arc length when curved by thermal deformation $l = r(2\theta)$, substitution of $\theta = \frac{1}{2}\frac{l}{r}$ into Eq. (3) gives

$$\varepsilon_{eff} = \ln \frac{2 \sin\left(\frac{1}{2}\frac{l}{r}\right) + \frac{h}{l}\frac{l}{r}\cos\left(\frac{1}{2}\frac{l}{r}\right)}{\frac{l}{r}\left(1 + \frac{h}{l}\right)} \tag{4a}$$

where

$$\frac{l}{r} = \frac{24(\alpha_1 - \alpha_2)dT}{\frac{h}{l}\left(14 + \frac{E_1}{E_2} + \frac{E_2}{E_1}\right)} \tag{4b}$$

and therefore

$$\alpha_{eff} = \frac{1}{dT}\ln \frac{2 \sin\left(\frac{1}{2}\frac{l}{r}\right) + \frac{h}{l}\frac{l}{r}\cos\left(\frac{1}{2}\frac{l}{r}\right)}{\frac{l}{r}\left(1 + \frac{h}{l}\right)} \tag{5}$$

As such, the effective thermal strain, and hence the effective CTE, can be calculated if the materials of the bimetal $(\alpha_1, \alpha_2, E_1, E_2)$, the change in temperature dT, and the dimensionless thickness of the bimetallic strip h/l are known *a priori*. The above thermal strain calculation applies for converting the originally square grid into the ones that reflect the Islamic geometric pattern shown in Fig. 1 (top). The proof of concept on the validity of bimetallic strips—specifically the deflection of a single bimetallic strip—to act as structural elements within a metamaterial has been verified via experimentation and finite element method by Li et al. [22].

The terminal deformation is a special case that is defined when the convex surfaces from two opposing sides of a unit cell come into contact with one another to reflect the Islamic geometric pattern displayed in Fig. 1 (bottom). A schematic for analysis is displayed in Fig. 4. It must be borne in mind that the terminal deformation as defined herein does not imply that further thermal deformation is arrested. In fact, further deformation can still be obtained upon attainment of terminal deformation; however, the shape of the curved bimetallic strip is no longer confined to a circular arc. In other words, the terminal deformation defined herein is the final stage of deformation at which the bimetallic strip conforms to a circular arc. With reference to Fig. 4, the distance between the centers of two nearest square blocks is at the minimum,

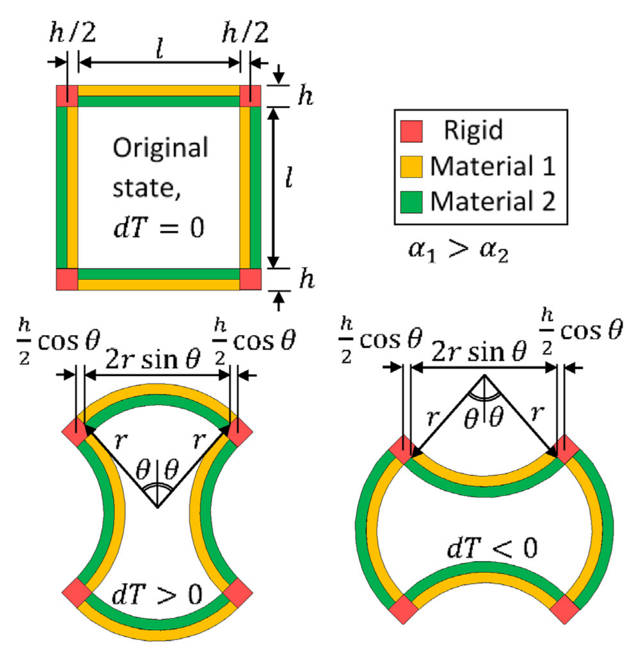

Fig. 3. Depiction of a unit cell at original state (top left) undergoing deformation due to heating (bottom left) and cooling (bottom right) for analysis.

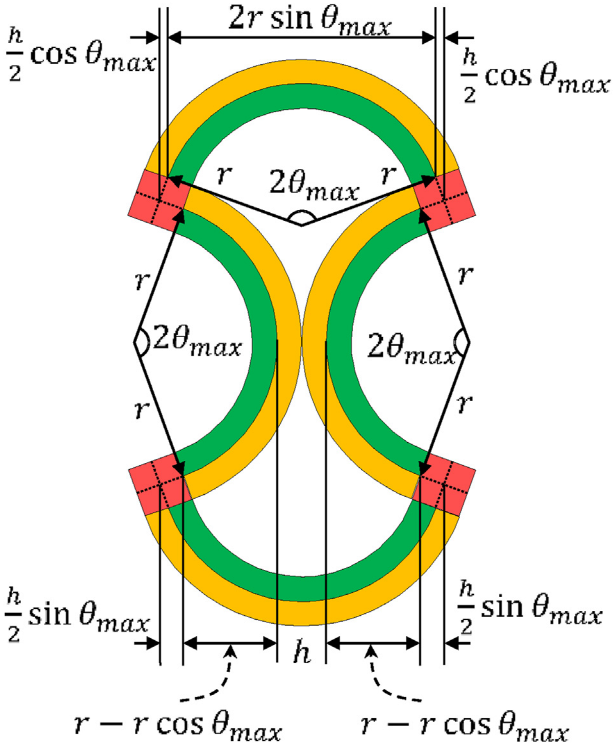

Fig. 4. A fully-curved unit cell for analysis of terminal deformation.

l_{min}. This minimum distance can be obtained by considering the top circular arc to give $l_{min} = 2r\sin\theta_{max} + h\cos\theta_{max}$. Alternatively, the same minimum distance can also be obtained by considering the left and right circular arcs that are in contact to give $l_{min} = 2r(1 - \cos\theta_{max}) + h(1 + \sin\theta_{max})$. Equating these two descriptions of l_{min}, we have

$$\frac{2 - \frac{h}{r}}{2 + \frac{h}{r}}\sin\theta_{max} + \cos\theta_{max} = 1 \tag{6a}$$

where

$$\frac{h}{r} = \frac{24(\alpha_1 - \alpha_2)dT}{14 + \frac{E_1}{E_2} + \frac{E_2}{E_1}} \tag{6b}$$

Since $0^\circ < \theta_{max} < 90^\circ$, Eq. (6a) implies two theoretical solutions for θ_{max}. The lower solution, $\theta_{max} = 0^\circ$, corresponds to the original state, and is therefore discarded in favor of the upper solution wherein $\lim_{h\to 0}\theta_{max} = \pi/2$ for diminishing bimetal strip thickness.

3. Results and discussion

The expression for the effective thermal strain described by Eq. (4) can be simplified by employing the first two terms of the sine and cosine series expansions so that

$$\frac{2\sin\theta + \frac{h}{l}\frac{l}{r}\cos\theta}{\frac{l}{r}\left(1 + \frac{h}{l}\right)} \approx 1 - \frac{1}{8}\frac{l^2}{r^2}\left(\frac{\frac{1}{3} + \frac{h}{l}}{1 + \frac{h}{l}}\right) \approx 1 - \frac{1}{24}\frac{l^2}{r^2} \tag{7}$$

for negligible dimensionless thickness h/l of the bimetallic strip. Substitution of Eq. (7) into Eq. (4) leads to

$$\varepsilon_{eff} \approx \ln\left(1 - \frac{1}{24}\frac{l^2}{r^2}\right) \approx -\frac{1}{24}\frac{l^2}{r^2} = -\frac{24(\alpha_1 - \alpha_2)^2}{\frac{h^2}{l^2}\left(14 + \frac{E_1}{E_2} + \frac{E_2}{E_1}\right)^2}(dT)^2 \tag{8}$$

that is, the effective thermal strain approximates a quadratic function with respect to the change in temperature. It follows that the effective CTE for the approximate model

$$\alpha_{eff} \approx -\frac{24(\alpha_1 - \alpha_2)^2}{\frac{h^2}{l^2}\left(14 + \frac{E_1}{E_2} + \frac{E_2}{E_1}\right)^2}dT \tag{9}$$

varies linearly with the change in temperature.

The datasets adopted herein are $\alpha_1 = 17 \times 10^{-6}K^{-1}$ and $E_1 = 117GPa$ for the copper layer of the Copper-Steel bimetallic strip, and $\alpha_1 = 19 \times 10^{-6}K^{-1}$ and $E_1 = 112.5GPa$ for the brass layer of the Brass-Steel bimetallic strip. For both bimetallic strips, the properties used for the steel layer are $\alpha_2 = 12 \times 10^{-6}K^{-1}$ and $E_2 = 200GPa$. Fig. 5 shows the plots of persistently effective negative thermal strain of the composite metamaterial regardless of whether the temperature increases or decreases, whereby the continuous curves were plotted using the exact model described by Eq. (4) while the discrete points refer to the approximate model furnished in Eq. (8). The family of effective CTEs of the composite metamaterials, as a function of temperature change, are displayed in Fig. 6 whereby the continuous lines for the exact model were plotted using Eq. (5) while the discrete points for the linearized model were calculated based on Eq. (9). It suggests that the effective CTE exhibits positive CTE with cooling from the original state but reverses to NTE behavior upon heating from the original state. In spite of the numerous simplifications implemented for the effective thermal strain, the approximate model correlates well with the exact model. Specifically the magnitudes of the approximated effective thermal strain and the effective CTE models underestimate those of the exact models by about 1% for $h/l = 0.005$, 2% for $h/l = 0.010$, 2.9% for $h/l = 0.015$, and 3.8% for $h/l = 0.020$ for the considered bimetallic strips and range of temperature change.

The maximum rotation θ_{max} of the rigid square blocks can be calculated firstly by substituting the material properties of the bimetal layers and the temperature change into Eq. (6b) to yield the h/r ratio, which can then be substituted into Eq. (6a). The maximum rotation of the rigid squares when $dT = 100K$ is $\theta_{max} = 89.96^\circ$ for the Copper-Steel bimetallic strip and $\theta_{max} = 89.94^\circ$ for the Brass-Steel bimetallic strip. Even if the change in temperature increases to $dT = 200K$, the maximum rotations are $\theta_{max} = 89.92^\circ$ and $\theta_{max} = 89.88^\circ$ for the Copper-Steel and the Brass-Steel bimetallic strips, respectively. Due to the very small percentage error in comparison to the idealized case of negligible bimetallic strip thickness, the simplifying assumption of $\theta_{max} = 90^\circ$ is valid for temperature change within the practical range, thereby indicating the possibility of the composite metamaterials to attain the Islamic geometric pattern of Fig. 1 (bottom).

Throughout the entire modeling it has been assumed that upon a change in temperature, each straight bimetallic strip transforms into a curve with consistent curvature, i.e. curved bimetallic strip conforms to the arc of a circle. If the surrounding temperature is not uniformly distributed at the local scale, the resulting curve does not conform to the arc of a circle. This gives two possible consequences. Firstly, the distance L_f is no longer accurate, thereby limiting the accuracy of ε_{eff} and hence that of α_{eff}. Secondly, accuracy of the quantitative descriptions of l_{mim} and θ_{max} are affected. It is more likely, however, for the temperature distribution to be non-uniform

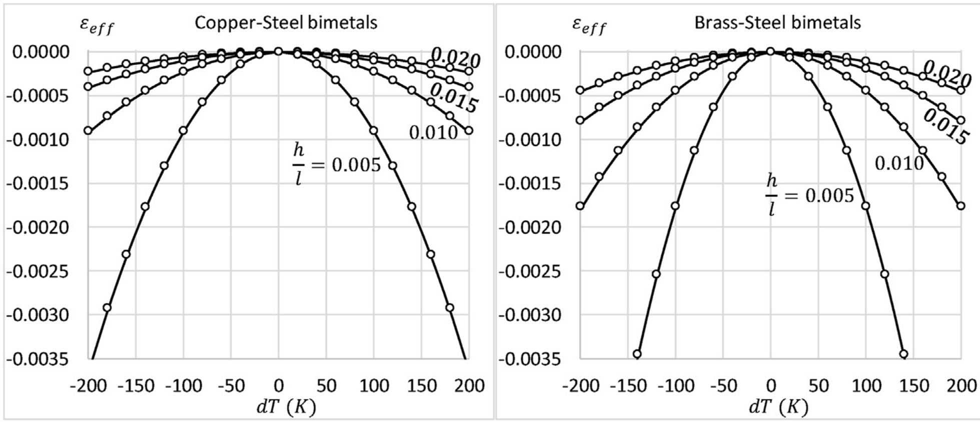

Fig. 5. Plots of effective thermal strain of the composite metamaterial with Copper-Steel bimetallic strip (left) and Brass-Steel bimetallic strip (right) using exact model (curves) and approximate model (circles).

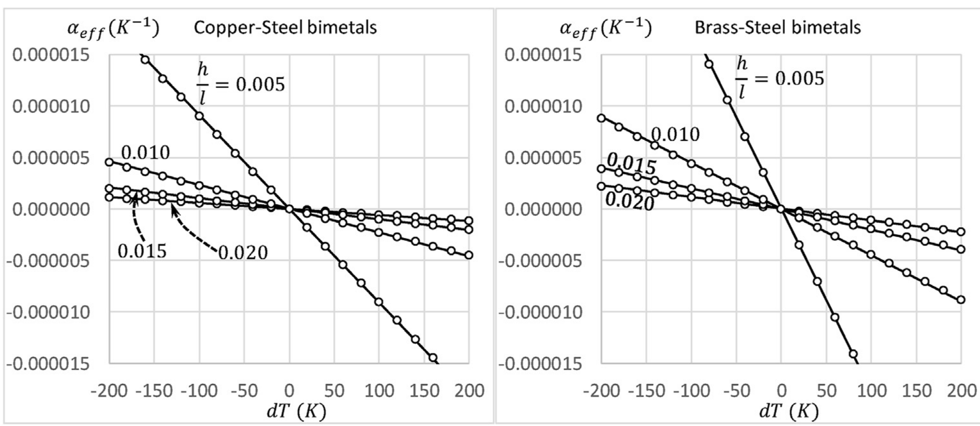

Fig. 6. Plots of effective CTE for the composite metamaterial incorporating Copper-Steel bimetallic strip (left) and Brass-Steel bimetallic strip (right) based on exact model (lines) and approximate model (circles).

at the global scale. The arising non-uniform distortion of cells across the entire metamaterial structure would, therefore, introduce additional internal stresses. The internal stresses within the bimetallic strips are not of concern, as observations on practical applications do not exhibit delamination therein. However, there is valid concern regarding internal stresses generated between the ends of the bimetallic strips and the rigid blocks. These internal stresses can be largely prevented by ensuring that the constructed system is of square array and not rectangular array. Since it is known that the resulting curvature is the same for all the bimetallic strips, the angular changes at the ends of the horizontal and vertical bimetallic strips are equal if both sets of strips are of equal length. This means that the rotational angle of the rigid blocks due to the curving of the horizontal strips is equal to that due to the curving of the vertical strips, thereby preventing internal stresses at the built-in ends. Nevertheless, a small amount of internal stresses may still arise at the built-in ends due to imperfections. This can be greatly reduced by applying structural adhesive, which is known to manifest high strength and low modulus permanent bond, between the ends of the bimetallic strips and the rigid blocks.

Hence the role of materials nature — in the form of the bimetallic strip — is to increase the magnitude of the CTE significantly by taking advantage of the ease of curving in response to temperature change. The configuration design — in the form of the square array — not only prevents build-up of the internal stresses but also contributes towards low weight arising from the low porosity.

4. Conclusions and recommendation

Inspired by Islamic geometrical patterns found in Spain, a metamaterial that incorporates bimetallic strips has been fashioned such that these patterns are concealed in their original state but are fully manifested upon a temperature change. In addition to a change in the sign of CTE, the metamaterial demonstrates adjustability of the CTE magnitude that is linearly correlated with the change in temperature and in-plane isotropy of the effective CTE. Specifically, (a) $\alpha_{eff} < 0$ for $dT > 0$, (b) $\alpha_{eff} > 0$ for $dT < 0$, and (c) $|\alpha_{eff}| \propto |dT|$. Chiral structures exhibit negative Poisson's ratio (auxetic) properties [23,24]. Due to its resemblance of the anti-tetrachiral structure, an investigation of this metamaterial's auxeticity upon temperature change is suggested for future work.

Declaration of competing interest

The author declares that he has no known competing financial interests or personal relationships that could have appeared to influence the work reported in this paper.

References

[1] J.S.O. Evans, J.C. Hanson, A.W. Sleight, Room-temperature superstructure of ZrV_2O_7, Acta Crystallogr. B 54 (6) (1998) 705–713.
[2] M.P. Attfield, A.W. Sleight, Exceptional negative thermal expansion in $AlPO_4$–17, Chem. Mater. 10 (7) (1998) 2013–2019.

[3] D.A. Woodcock, P. Lightfoot, L.A. Villaescusa, M.J. Diaz-Cabanas, M.A. Camblor, D. Engberg, Negative thermal expansion in the siliceous zeolites chabazite and ITQ-4: a neutron powder diffraction study, Chem. Mater. 11 (9) (1999) 2508−2514.
[4] E. Zhang, R. Chen, C. Huang, J. Yu, K. Zhang, W. Wang, S. Liu, J. Ling, X. Wan, H.Z. Lu, F. Xiu, Tunable positive to negative magnetoresistance on atomically thin WTe2, Nano Lett. 17 (2) (2017) 878−885.
[5] P.F. Wang, Y. Liu, J. Yin, W. Ma, Z. Dong, W. Zhang, J.L. Zhu, J.L. Sun, A tunable positive and negative photoconductive photodetector based on a gold/graphene/p-type silicon heterojunction, J. Mater. Chem. C 7 (4) (2019) 887−896.
[6] J.F. Algorri, P. Morawiak, N. Bennis, D.C. Zografopoupos, V. Urruchi, L. Rodriguez-Cobo, L.R. Jaroszewicz, J.M. Sanchez-Pena, J.M. Lopez-Higueta, Positive-negative tunable liquid crystal lenses based on a microstructured transmission line, Scient, Rep 10 (2020) 10153.
[7] C.S. Ha, M.E. Plesha, R.S. Lakes, Simulations of thermoplastic triangular cell lattices with bonded joints by finite element analysis, Extreme Mech. Lett. 12 (2017) 101−107.
[8] L. Wu, B. Li, J. Zhou, Isotropic negative thermal expansion metamaterials, Appl. Mater. Interfaces 8 (27) (2016) 17721−17727.
[9] T.C. Lim, 2D metamaterial with in-plane positive and negative thermal expansion and thermal shearing based on interconnected alternating bimaterials, Mater. Res. Express 6 (11) (2019) 115804.
[10] T.C. Lim, Composite metamaterial with sign-switchable coefficients of hygroscopic, thermal and pressure expansions, Adv. Compos. Hybrid. Mater. 2 (4) (2019) 657−669.
[11] T.C. Lim, Metamaterials with Poisson's ratio sign toggling by means of microstructural duality, SN Appl. Sci. 1 (2) (2019) 176.
[12] T.C. Lim, A 2D auxetikos system based on interconnected shurikens, SN Appl. Sci. 1 (11) (2019) 1383.
[13] A. Rafsanjani, D. Pasini, Multistable compliant auxetic metamaterials inspired by geometric patterns in Islamic arts, Bull. Am. Phys. Soc. 61 (2016) K40.00008.
[14] A. Rafsanjani, D. Pasini, Bistable auxetic mechanical metamaterials inspired by ancient geometric motifs, Extreme Mech. Lett. 9 (2016) 291−296.
[15] T.C. Lim, Composite metamaterial square grids with sign-flipping expansion coefficients leading to a type of Islamic design, SN Appl. Sci. 2 (5) (2020) 918.
[16] T.C. Lim, Metacomposite structure with sign-changing coefficients of hygrothermal expansions inspired by Islamic motif, Compos. Struct. 251 (2020) 112660.
[17] T.C. Lim, A perfect 2D auxetic sliding mechanism based on an Islamic geometric pattern, Eng. Res. Express 3 (1) (2021), 015025.
[18] T.C. Lim, An auxetic system based on interconnected Y-elements inspired by Islamic geometric patterns, Symmetry 13 (5) (2021) 865.
[19] T.C. Lim, Aspect ratio and size effects of a metacomposite with interconnected Y-elements, J. Phys.: Conf. Ser. 2047 (2021), 012029, https://doi.org/10.1088/1742-6596/2047/1/012029.
[20] T.C. Lim, A class of shape-shifting composite metamaterial honeycomb structures with thermally-adaptive Poisson's ratio signs, Compos. Struct. 226 (2019) 111256.
[21] T.C. Lim, Adjustable positive and negative hygrothermal expansion metamaterial inspired by the Maltese cross, Roy. Soc. Open Sci. 8 (8) (2021) 210593.
[22] D. Li, J. Ma, L. Dong, R.S. Lakes, A bi-material structure with Poisson's ratio tunable from positive to negative via temperature control, Mater. Lett. 181 (2016) 285−288.
[23] K.K. Dudek, New type of rotation of chiral mechanical metamaterials, Smart Mater. Struct. 29 (11) (2020) 115027.
[24] L. Mizzi, A. Spaggiari, Chiralisation of Euclidean polygonal tessellations for the design of new auxetic metamaterials, Mech. Mater. 153 (2021) 103698.